Magnetic field evolution in neutron stars

Ankan Sur

Email: ankansur@camk.edu.pl

Magnetic field in neutron stars

- Strongest
- Population
- Evolution and formation
- Energetic phenomena ranging from solar flares to gamma-ray and fast radio bursts

Magnetic field in neutron stars

- Control spin-down
- Dipole-emits EM radiation

$$B = \frac{3n^i(n_j m^j) - m^i}{r^3}$$

- Rotation causes electric potential at poles

  -extract particles and fill NS magnetosphere

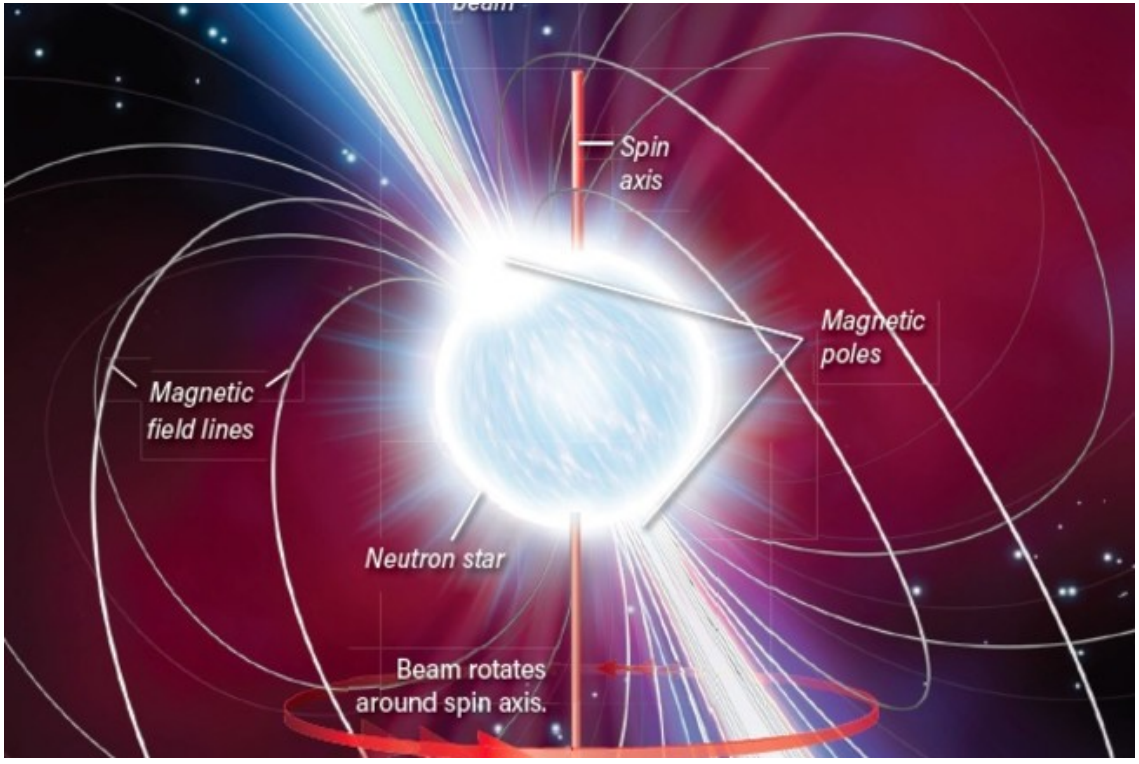

Inclination angle

- Inclination angle evolves as

$$\frac{d\alpha}{dt} = -k_2 \beta \frac{B_p^2}{P^2} \sin\alpha \cos\alpha$$

- Radio polarisation shows evolution in 10^7 years.
- In magnetars

$$\dot{\alpha} = \frac{\dot{E}_{\rm visc}}{I\epsilon \sin\alpha \cos\alpha \Omega^2} + \frac{\dot{E}_{\rm EM}}{I\Omega^2}$$

Orthogonalization Alignment

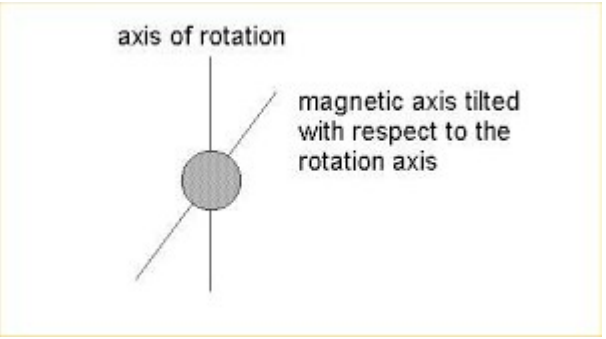

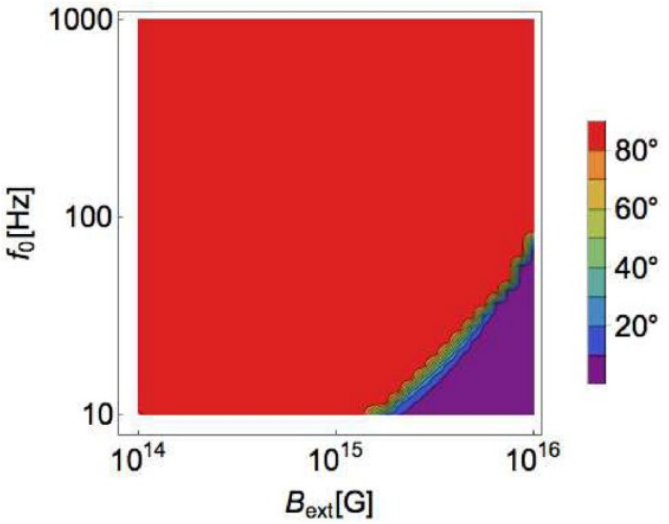

Lander (MNRAS 2020)

Spin period and magnetic field

- By timing pulsars individually, usually expressed as a Taylor series

$$P(t) = P(t_0) + \left.\frac{dP}{dt}\right|_{t_0}(t - t_0) + \left.\frac{d^2P}{dt^2}\right|_{t_0}(t - t_0)^2 + \ldots.$$

- Electromagnetic radiation = decrease in rotational energy

$$\dot{\omega} = -\frac{1}{6c^3}\frac{B_s^2 R^6}{I}\sin^2\alpha\omega^3$$

- The strength of magnetic field can be estimated

$$B_s = 3 \times 10^{11}\sqrt{\frac{P}{10\,\mathrm{ms}}\frac{\dot{P}}{10^{-14}}}\,\mathrm{G}$$

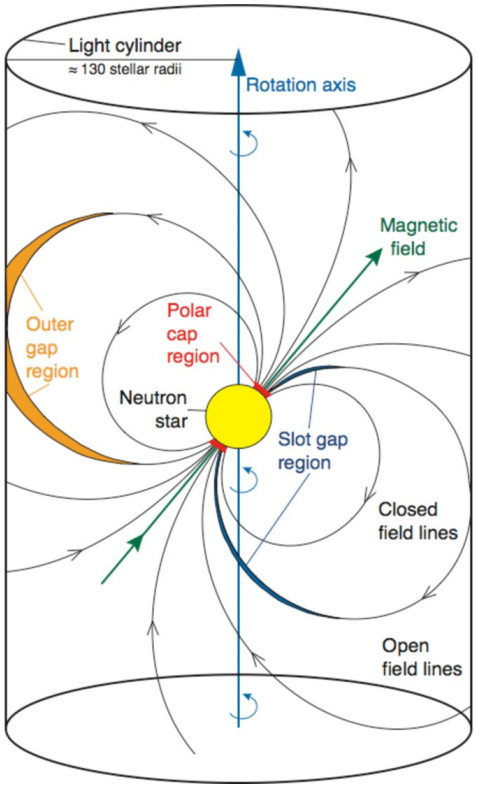

Credits: Handbook of Pulsar Astronomy by Duncan Ross Lorimer and Michael Kramer

Some parameters

- Characteristic age

$$\tau_c \propto \frac{P}{\dot{P}}$$

- Luminosity

$$L \propto \frac{\dot{P}}{P^3}$$

- Field strength

$$B_s \propto \sqrt{P\dot{P}}$$

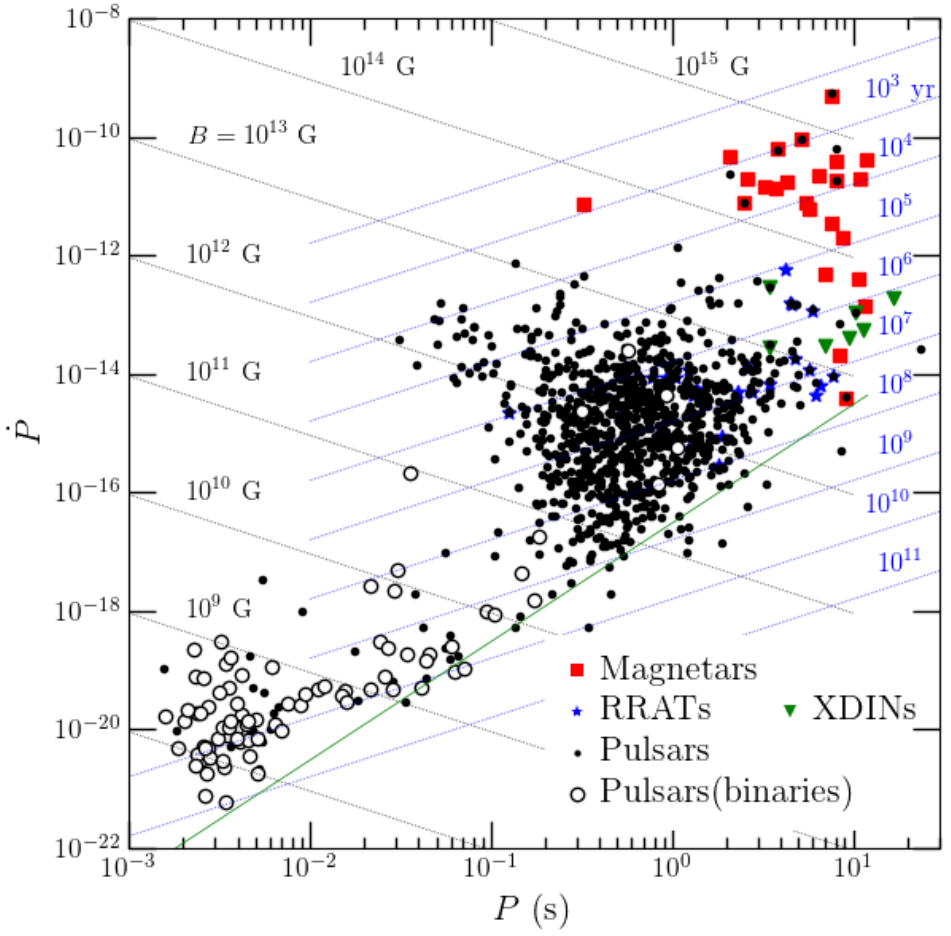

Braking index

- One of the characteristics which is used to study magnetic field evolution is the braking index

$$n = 2 - \frac{P\ddot{P}}{\dot{P}^2}$$

- If the dipole field and obliquity angle do not evolve in time, it is expected that n = 3.
- If the field is multipolar, with dominant component l, the braking index is n = 2l + 1
- The braking index could therefore be a powerful tool to study both the configuration and evolution of NS magnetic fields

PSR	n	Reference
B0531+21(Crab)	2.51(1)	Lyne et al. (1993)
B0540−69	2.14(1)	Livingstone et al. (2007)
B0833−45(Vela)	1.4(2)	Lyne et al. (1996)
J1119−6127	2.684(2)	Weltevrede et al. (2011)
B1509−58	2.839(1)	Livingstone et al. (2007)
J1734−3333	0.9(2)	Espinoza et al. (2011b)
J1833−1034	1.857(1)	Roy et al. (2012)
J1846−0258	2.65(1)	Livingstone et al. (2007)

Magnetic field geometry

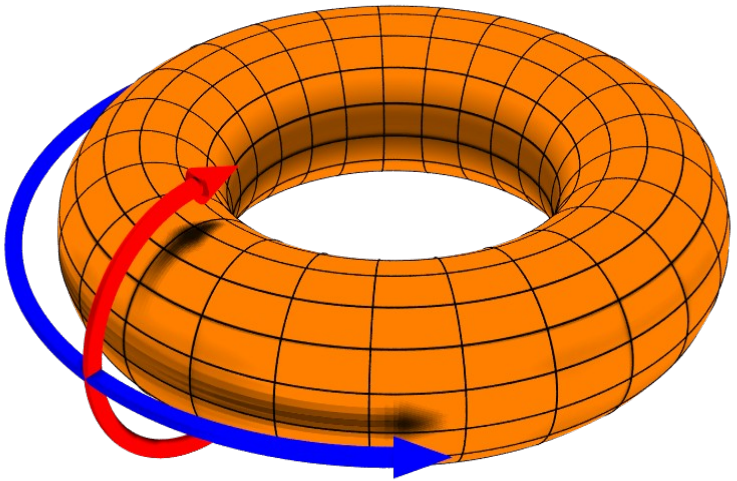

POLOIDAL MAGNETIC FIELD

TOROIDAL MAGNETIC FIELD

Role of poloidal and toroidal fields

- The presence of small-scale poloidal fields is often discussed as an essential mechanism which increases the curvature of open field lines, and thus leads to the activation of the pulsar mechanism in long-period radio pulsars.

- Toroidal magnetic fields can be present in the NS crust. This field component decays and heats the crust, increasing the total NS thermal flux, which seems to be a promising mechanism to explain magnetar quiescent emission.

- Large-scale toroidal magnetic field could also cause the magnetospheric twist in magnetars which leads to an increase in the magnetospheric currents, which is further seen in X-ray spectra because low-energy X-ray photons are scattered by these currents, which creates a power-law scaling at energies above $2 - 3$ keV.

Magnetic field from theory

- Magnetic field configuration is theorized using magnetohydrodynamical equilibrium calculations.
- Equilibrium: $\nabla P + \rho \nabla \phi_g = \frac{1}{c} \vec{J} \times \vec{B}$
- Solutions are not unique and it is unclear whether they are stable.
- MagnetoHydroDynamics : Maxwell+Fluid mechanics

$$\nabla \cdot \mathbf{E} = \frac{\rho}{\varepsilon_0}$$

$$\nabla \cdot \mathbf{B} = 0$$

$$\nabla \times \mathbf{E} = -\frac{\partial \mathbf{B}}{\partial t}$$

$$\nabla \times \mathbf{B} = \mu_0 \mathbf{j} + \frac{1}{c^2} \frac{\partial \mathbf{E}}{\partial t}$$

$$\rho \left(\frac{\partial v}{\partial t} + v \cdot \nabla v \right) = -\nabla p + \nabla \cdot T + f$$

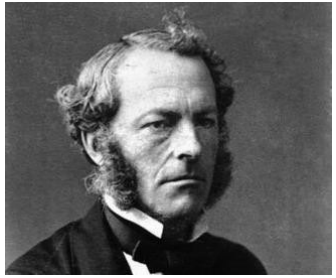

Stokes

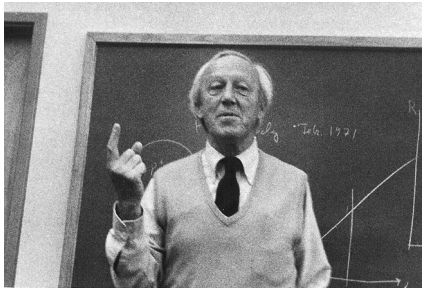

Alfven

Maxwell

Crustal field

Start with one of Maxwell's equations:

$$\frac{\partial B}{\partial t} = -c\nabla \times E$$

Supplemented this with Ohm's law:

$$\frac{\partial B}{\partial t} = -c\nabla \times \left(\frac{1}{4\pi e n_e}(\nabla \times B) \times B + \frac{c}{4\pi\sigma}\nabla \times B\right) \quad (9)$$

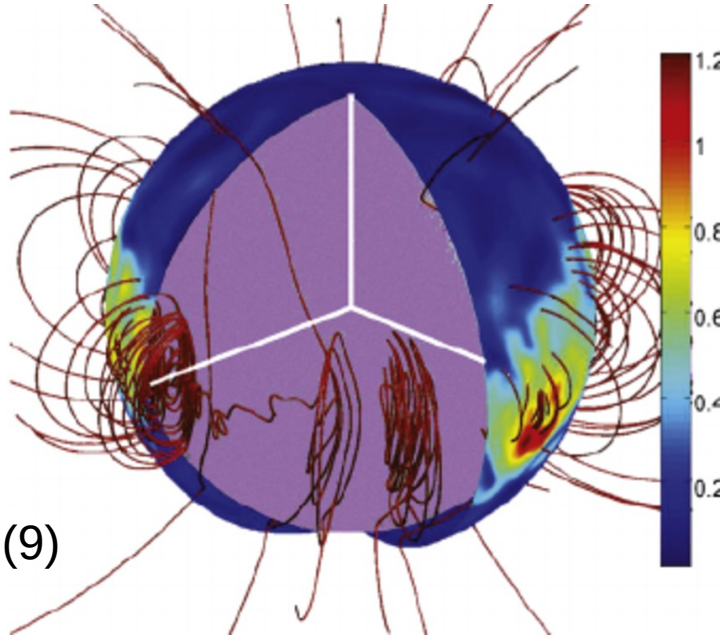

The first term on the right side of this equation corresponds to the **Hall effect**, and the second to the **Ohmic decay**.

Note also that the magnetic field which is being described here is the field within the NS itself, which cannot be directly measured

Crustal field: Ohm's Law

The partial differential eq. (9) can be solved analytically for some simple special cases. For example, pure Ohmic decay is described as:

$$\frac{\partial \vec{B}}{\partial t} = -\frac{c^2}{4\pi\sigma}\Delta\vec{B},$$

where $\nabla \times \nabla \times \vec{B} = \Delta\vec{B}$. If we decompose the field as a sum of poloidal and toroidal parts $\vec{B} = \vec{B}_p + \vec{B}_t$, the equation for the poloidal part becomes:

$$\frac{\partial \vec{B}_p}{\partial t} = -\frac{c^2}{4\pi\sigma}\Delta\vec{B}_p.$$

Crustal field: Ohm's Law

The toroidal part does not enter since Ohmic decay occurs separately. We can represent

$$\vec{B}_p(t,\vec{r}) = \vec{B}_0 \exp(i\omega t - \vec{k}.\vec{r})$$

Thus, we can simplify as

$$i\omega = -\frac{k^2 c^2}{4\pi\sigma}$$

If only magnetic field decay with the timescale $\tau_{\rm Ohm} = -\frac{1}{i\omega}$ for a field which has a spatial extent L = 1/k, we obtain

Thus, the magnetic field for pure Ohmic decay is

$$\vec{B}_p(t,\vec{r}) = \vec{B}_0(\vec{r}) \exp\left(-\frac{t}{\tau_{Ohm}}\right).$$

Crustal field: Ohm's Law

Conductivity is composed of phonons and crystalline impurities. The total conductivity can be written as

$$\sigma = \frac{\sigma_{ph}\sigma_Q}{\sigma_{ph} + \sigma_Q}$$

The timescales can be written as $\tau_{\rm Ohm}^{-1} = \tau_{\rm Ohm,ph}^{-1} + \tau_{\rm Ohm,Q}^{-1}$

The conductivity due to impurities $\sigma_{\rm Q} = 4.4 \times 10^{25}\ {\rm s}^{-1} \left(\frac{\rho_{14}^{1/3}}{Q}\right) \left(\frac{Y_e}{0.05}\right)^{1/3} \left(\frac{Z}{30}\right).$

The parameter Q characterises how ordered the crystalline structure of the crust.

The conductivity translates to a timescale of

$$\tau_{\rm Q} \approx 200\ {\rm Myr} \left(\frac{L}{1\ {\rm km}}\right)^2 \left(\frac{\rho_{14}^{1/3}}{Q}\right) \left(\frac{Y_e}{0.05}\right)^{1/3} \left(\frac{Z}{30}\right).$$

Crustal field:Ohm's Law

For the phonon conductivity

$$\sigma_{\rm ph} = 1.8 \times 10^{25}\ {\rm s}^{-1} \left(\frac{\rho_{14}^{7/6}}{T_8^2}\right)\left(\frac{Y_e}{0.05}\right)^{5/3},$$

The timescale which corresponds to this is

$$\tau_{\rm ph} \approx 80\ {\rm Myr} \left(\frac{L}{1\ {\rm km}}\right)^2 \left(\frac{\rho_{14}^{7/6}}{T_8^2}\right)\left(\frac{Y_e}{0.05}\right)^{5/3}.$$

In this way the magnetic field decay depends strongly on crustal temperature and becomes irrelevant when the NS cools down and reaches temperatures $T_8 < 0.1$ at ages $t > 1$ Myr.

Ohmic decay in the crust

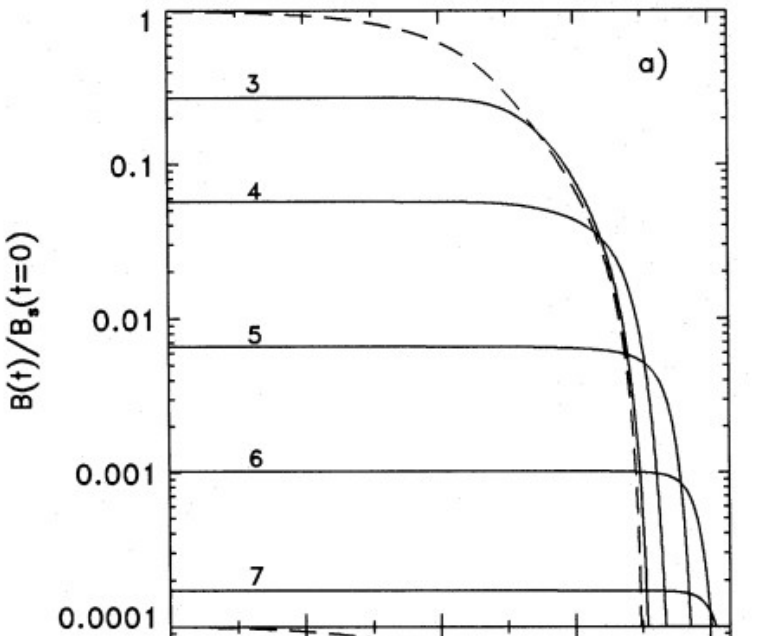

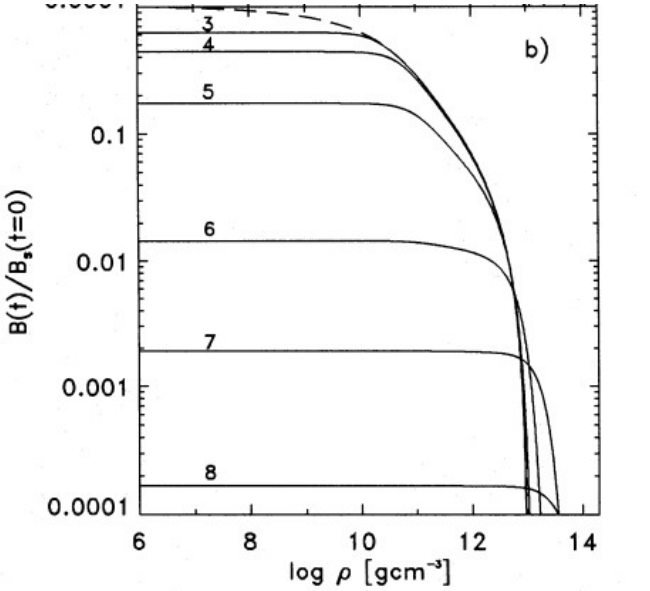

Figure 4. Evolution of the magnetic field distribution within the crust of the accretion-heated neutron star for standard (panel a) and accelerated (panel b) cooling. Shown is the radial component of the magnetic field, normalized to the initial field strength at the pole. Dashed lines show the initial field distributions. Numbers near the curves indicate the logarithm of the time.

Geppert, U (MNRAS 1994)

Crustal field: Hall effect

Hall evolution is more complicated.

Timescale of Hall: $$\tau_{\rm Hall} = \frac{4\pi e n_e L^2}{cB(t)}$$

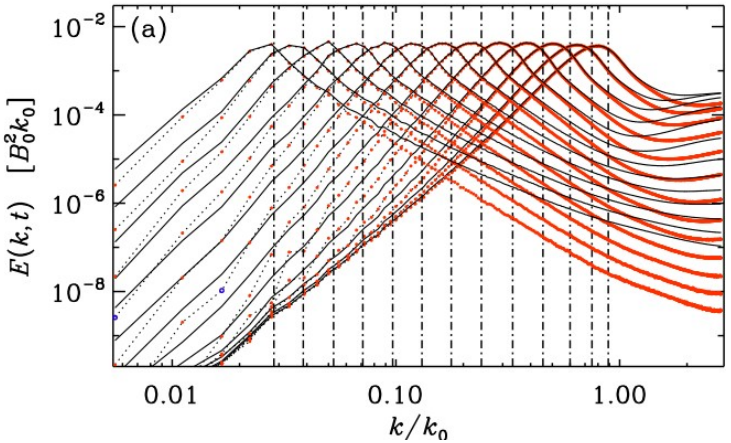

The Hall evolution is strongly nonlinear, coupling different spatial scales, and poloidal and toroidal components of the magnetic field together.

Any large-scale magnetic field would evolve through a cascade-like process towards smaller scales.

This behavior results in acceleration of the magnetic field decay, as the spatial scale L of electric currents decreases.

Crustal field: Hall effect

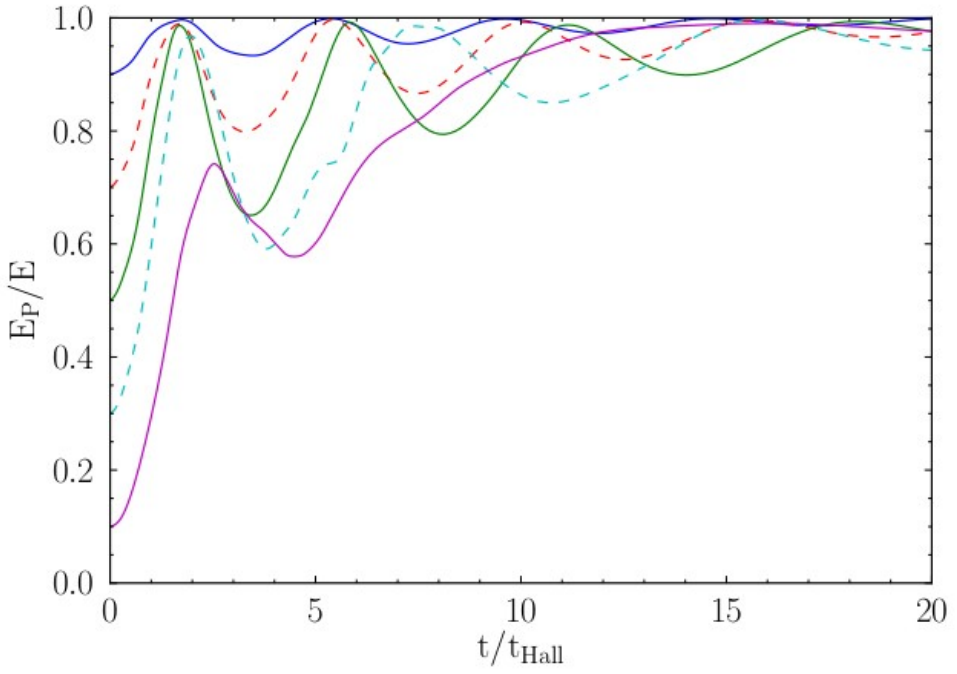

Figure 3. Evolution of the ratio E_P/E for simulations with different initial ratios, with initial conditions given by Eq. (8) with $R_B = 100$.

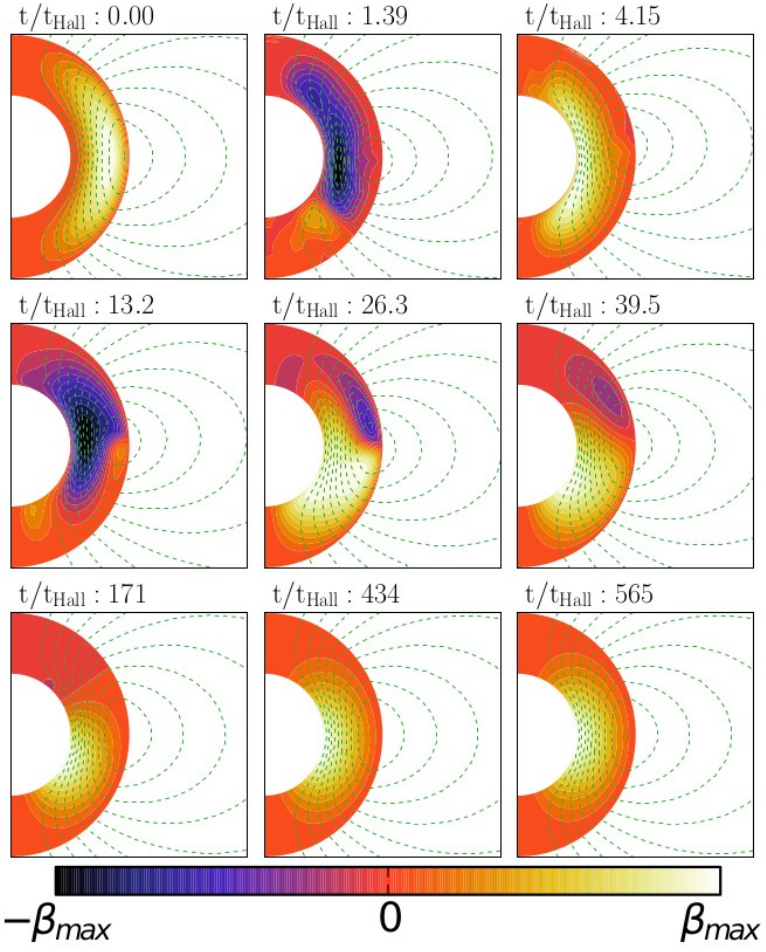

Merchant (ApJ 2014)

Field evolution in the crust

K.N. Gourgouliatos & A. Cumming MNRAS (2014)

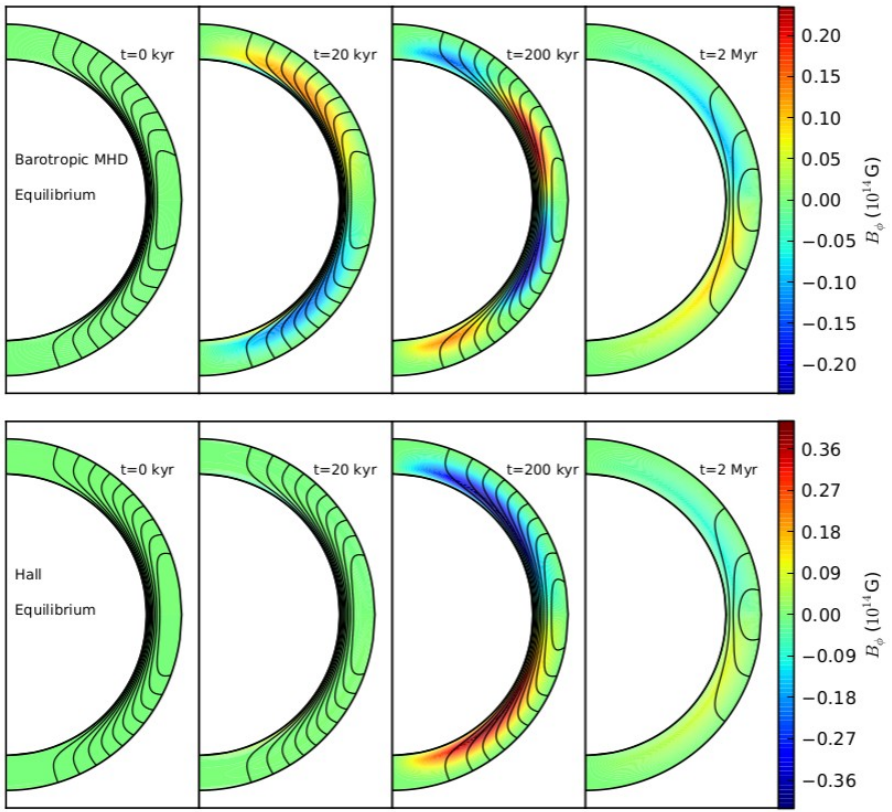

MHD

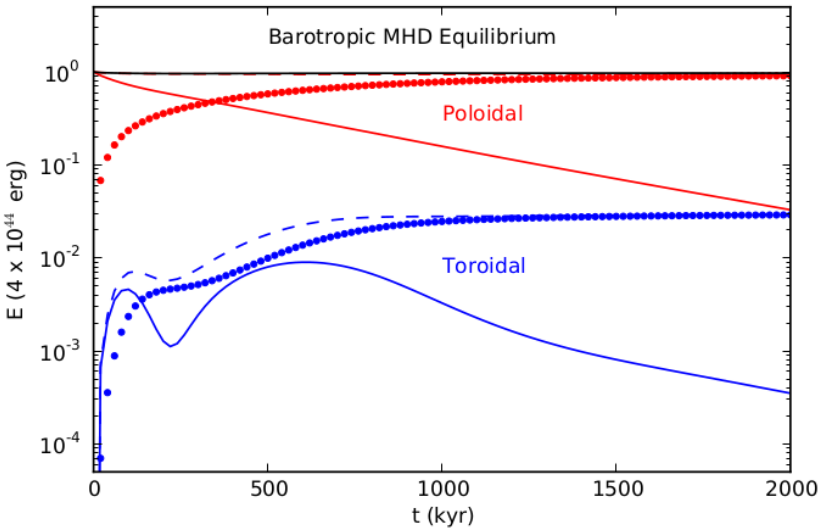

Figure 4. The energy of the various components of the field and Ohmic losses during the evolution of a field starting at barotropic MHD equilibrium. The red lines correspond to the poloidal field, the blue to the toroidal field, the solid lines correspond to the energy of the field, the dotted line is the time integrated Ohmic losses through poloidal or toroidal field, the dashed is the sum of the the solid and the dotted line of the respective colour, the total energy is plotted in black to demonstrate that the code is

Field evolution in the crust

K.N. Gourgouliatos & A. Cumming MNRAS (2014)

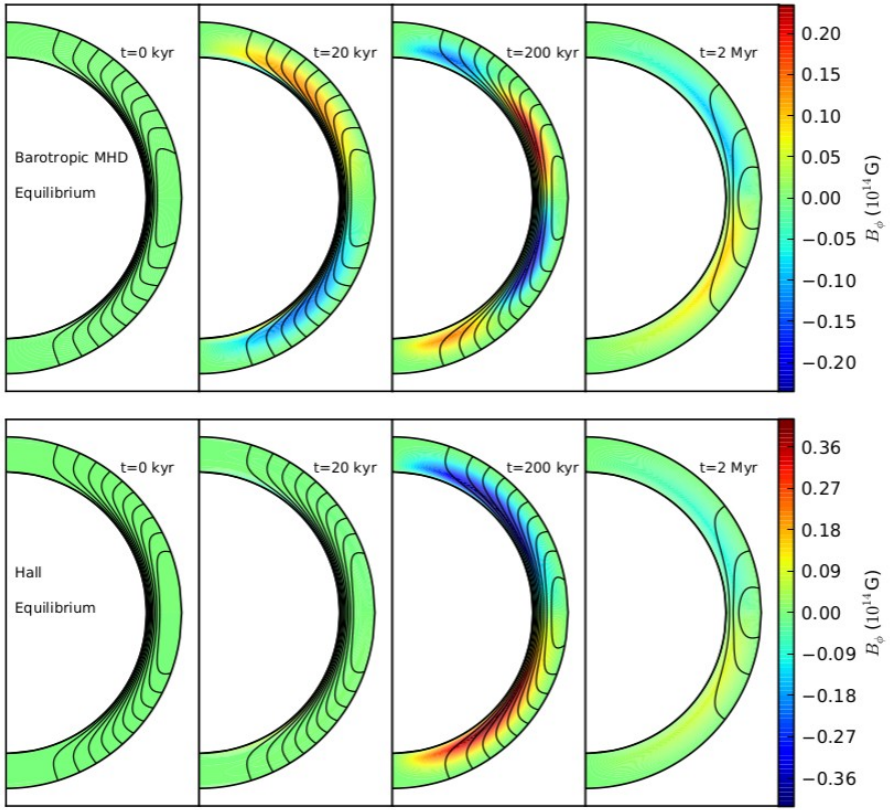

HALL

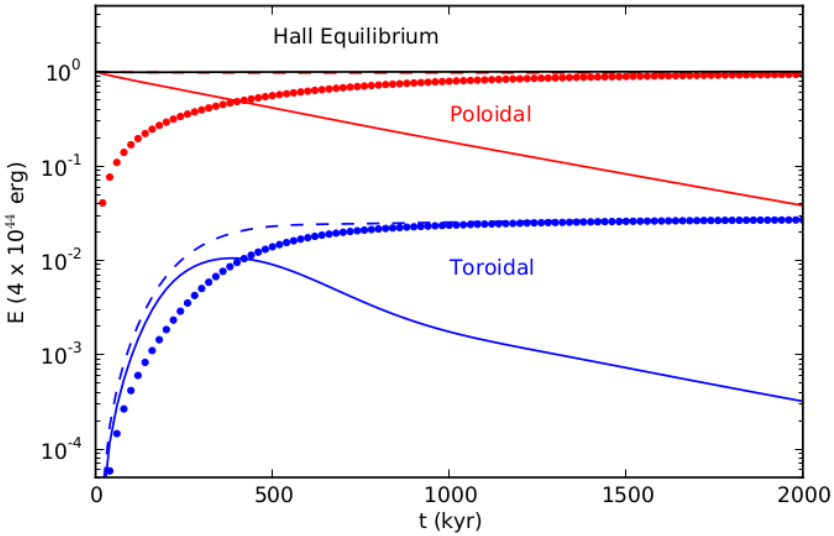

Figure 6. The energy of the various components of the field and Ohmic losses during the evolution of a field starting at Hall equilibrium, the colour and line coding is the same as in Figure 4. As the field starts in the state of Hall equilibrium it takes much longer to develop a significant toroidal component with the subsequent energetic behaviour similar to that of Figure 4.

Hall attractor

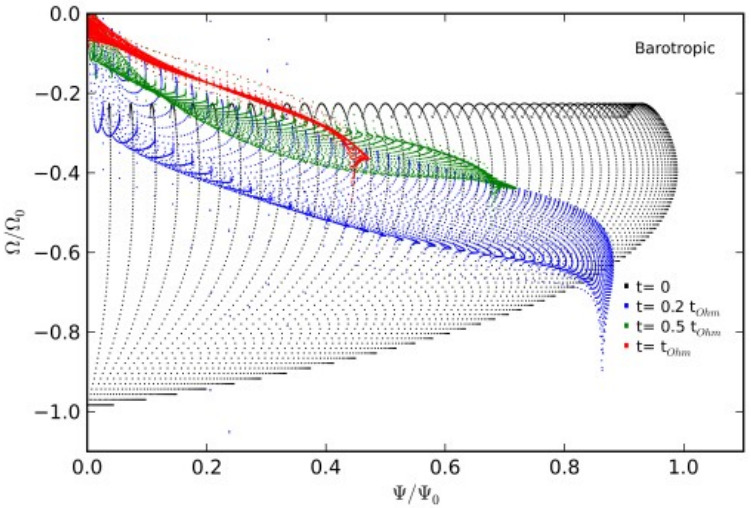

Initially there is differential rotation of the electron fluid along the field lines (black points), with multiple values of Ω for given Ψ, which after some Hall evolution tend to concentrate in a narrower region (blue and green points), and eventually the system saturates to isorotation (red points)

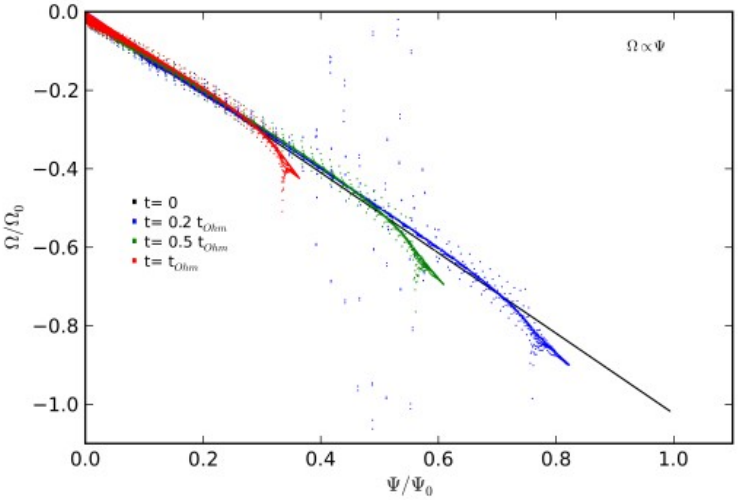

The scatter plot for a system starting with Ω = αΨ (black points), the initial structure is very close to the attractor state, thus the system changes only slightly its structure as shown with Ω and Ψ deviating from linearity (blue and green points), however the system maintains isorotation, even after a significant part of the field has been dissipated (red points).

Gourgouliatos & Cumming (PRL 2014)

Crust+core evolution

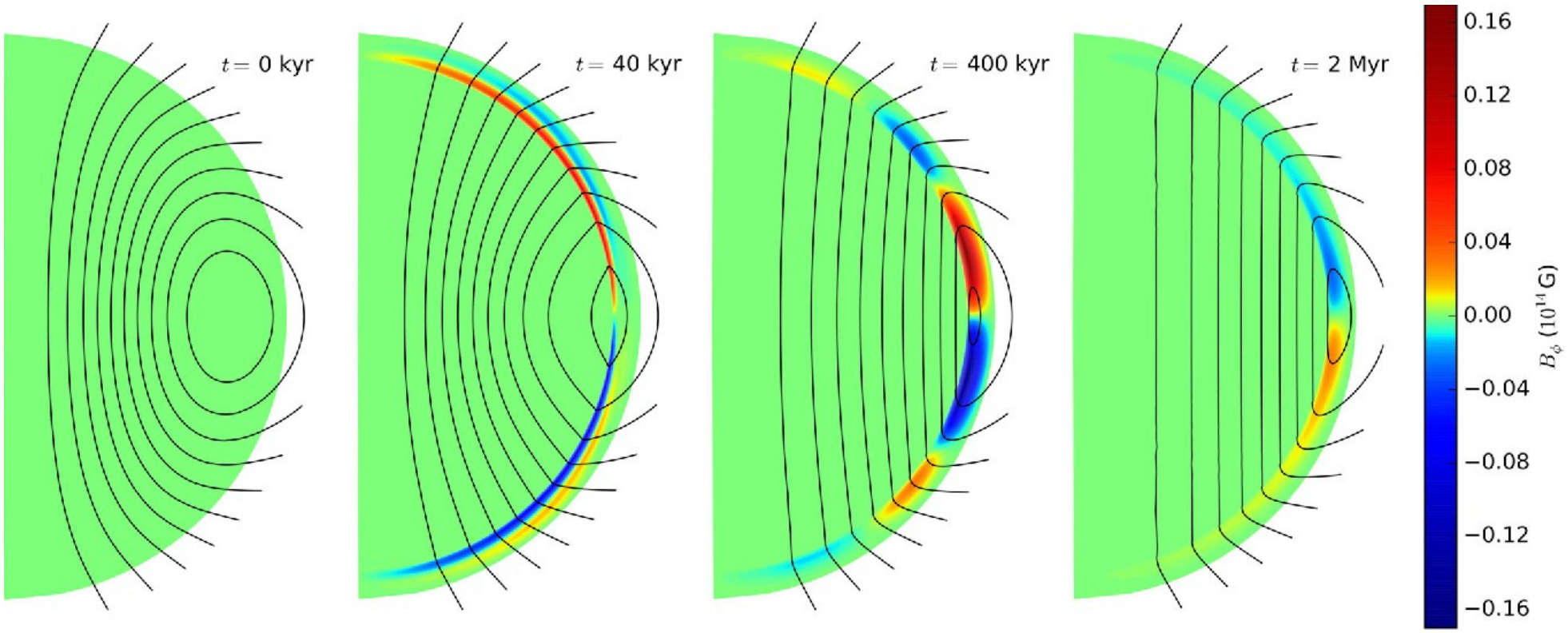

Hall + Ohmic (crust), Jones drift (core)

Bransgrove et al (2017)

Crust+core evolution

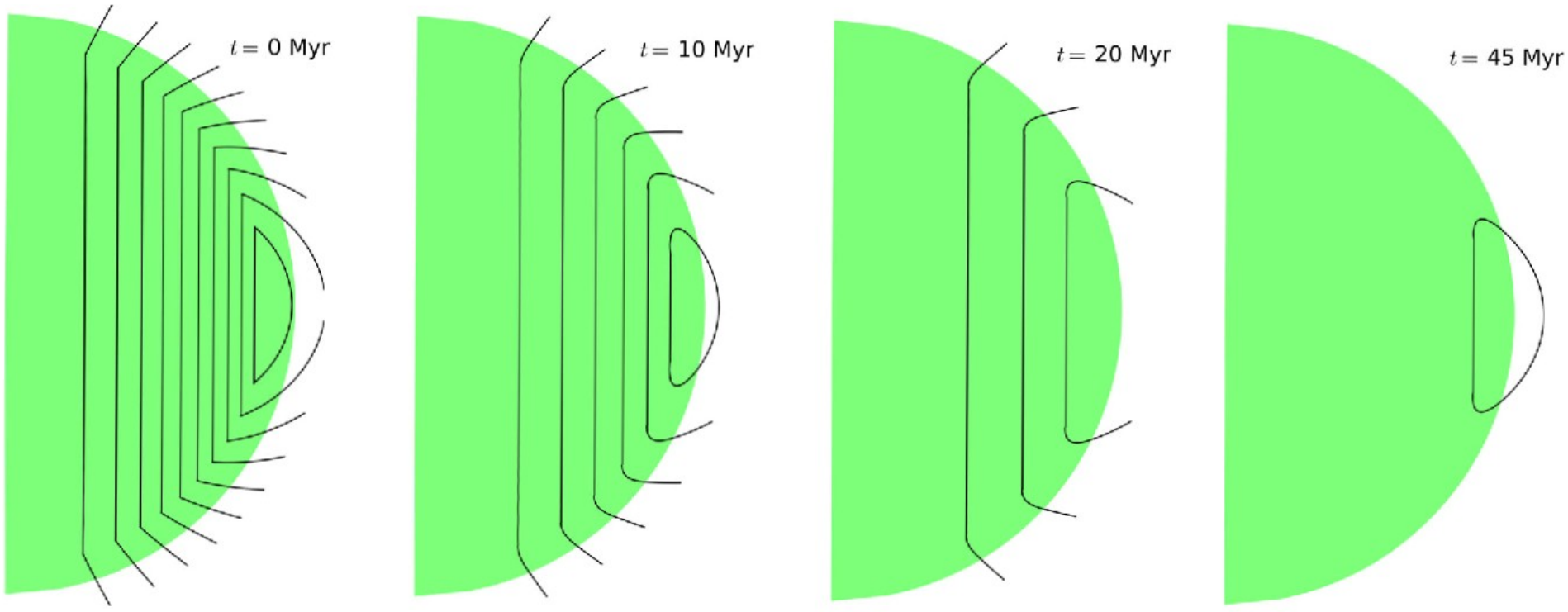

Ohmic (crust) + Jones drift (core)

Bransgrove et al (2017)

Axisymmetric equilibria

Euler equation $$0 = -\nabla P - \rho \nabla \Psi + \frac{1}{c}\mathbf{J} \times \mathbf{B},$$

Axisymmetric field $$\mathbf{B} = \mathbf{B}_{\rm pol} + \mathbf{B}_{\rm tor} = \nabla \alpha(r,\theta) \times \nabla \phi + \beta(r,\theta)\nabla \phi,$$

GS operator $$\Delta^\star = \frac{\partial}{\partial r^2} + \frac{\sin\theta}{r^2}\frac{\partial}{\partial \theta}\left(\frac{1}{\sin\theta}\frac{\partial}{\partial \theta}\right)$$

Grad-Shafranov equation

$$\Delta^* \alpha + \beta(\alpha)\beta'(\alpha) + \rho r^2 \sin^2\theta \chi'(\alpha) = 0,$$

Description of toroidal

$$\beta(\alpha) = \begin{cases} s(\alpha - \alpha_{\rm surf})^\lambda & \text{if} \quad \alpha \geq \alpha_{\rm surf} \\ 0 & \text{if} \quad \alpha < \alpha_{\rm surf}, \end{cases}$$

Armaza et.al(2015 ApJ)

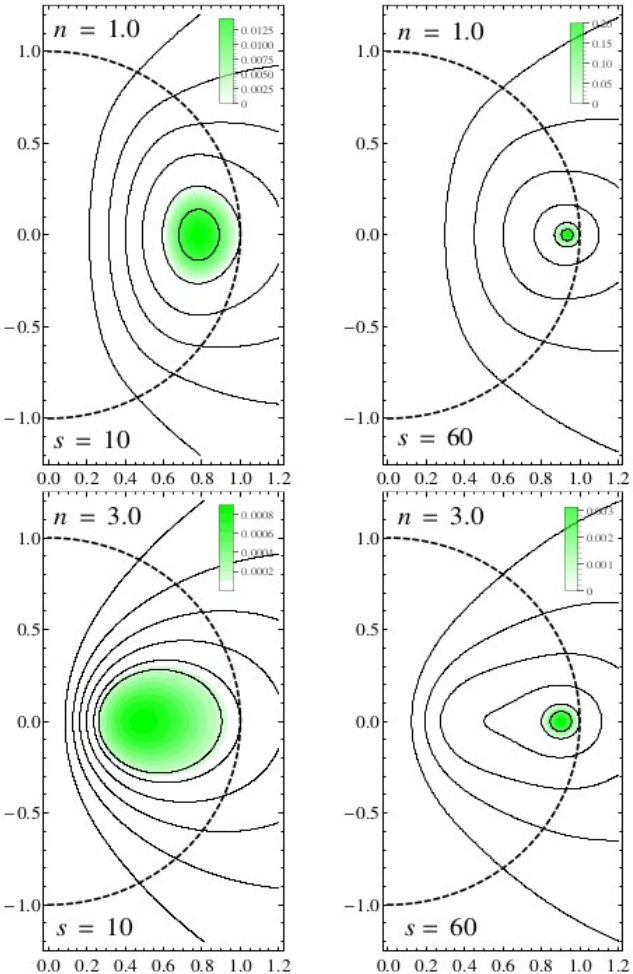

Axisymmetric equilibria

Lander, MNRAS 2009

Normal matter pulsar

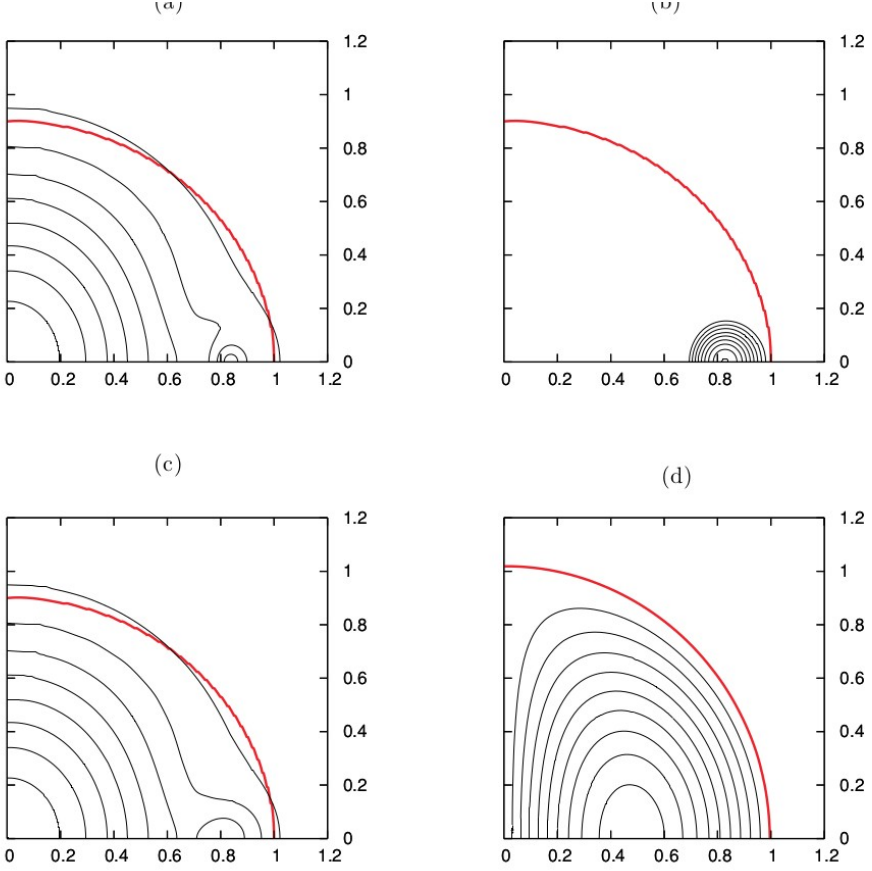

Superconducting core pulsar

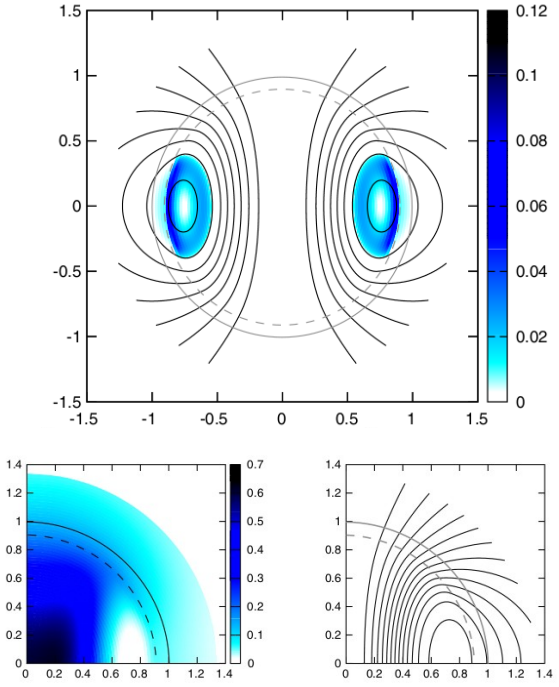

FIG. 1 (color online). Structure of a poloidal magnetic field in a superconducting star. On the left we show the magnitude of the field and on the right its direction (i.e., the field lines). The stellar surface R_* is indicated with the solid arc at a dimensionless radius of unity, while the dashed line at $0.9R_*$ shows the location of the crust-core boundary.

Lander, PRL 2013

Magnetic field from full 3D simulations

NEWTONIAN

- Ap stars - random initial field to stable ‘twisted-torus’ (Braithwaite & Nordlund 2006).

- stability of a possible poloidal field in neutron stars leads complete decay of the field (Braithwaite & Spruit 2006). Field evolves under diffusion, leads to crust cracking.

- formation of stable equilibria from turbulent initial conditions - existence of non-axisymmetric equilibria (Braithwaite 2008).

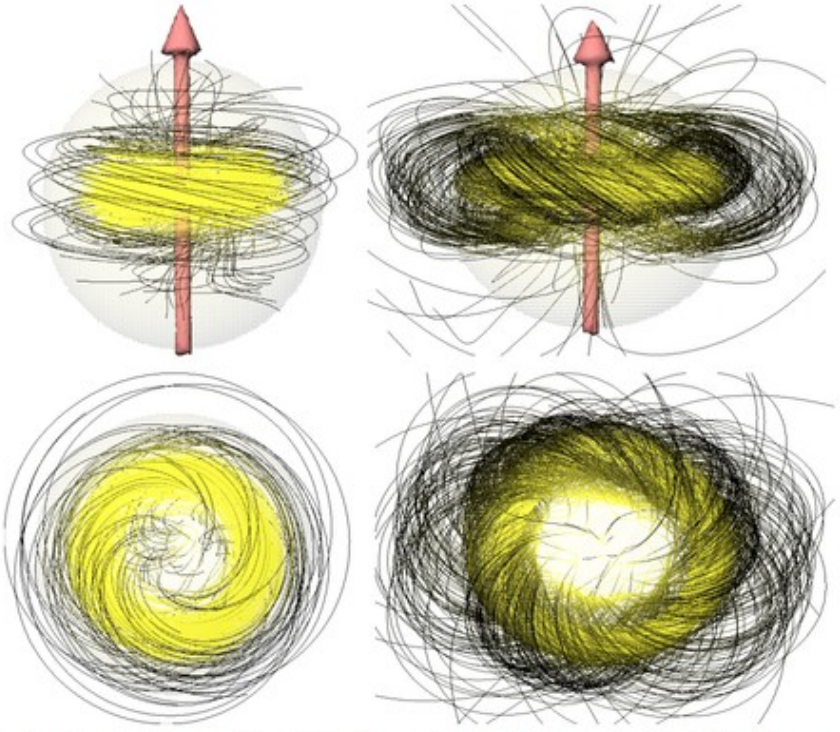

Braithwaite & Nordlund, 2006

Magnetic field from full 3D simulations

RELATIVISTIC

- In General Relativity, equilibrium configurations were obtained by Ciolfi et al (2010,2012,2013), Lasky et al (2011).
- These are the first non-axisymmetric equilibria attained with a polytropic equation of state.
- The evolution is dominated by the kink instability, which causes a cataclysmic reconfiguration of the magnetic field.
- Formation of quasi-equilibrium.

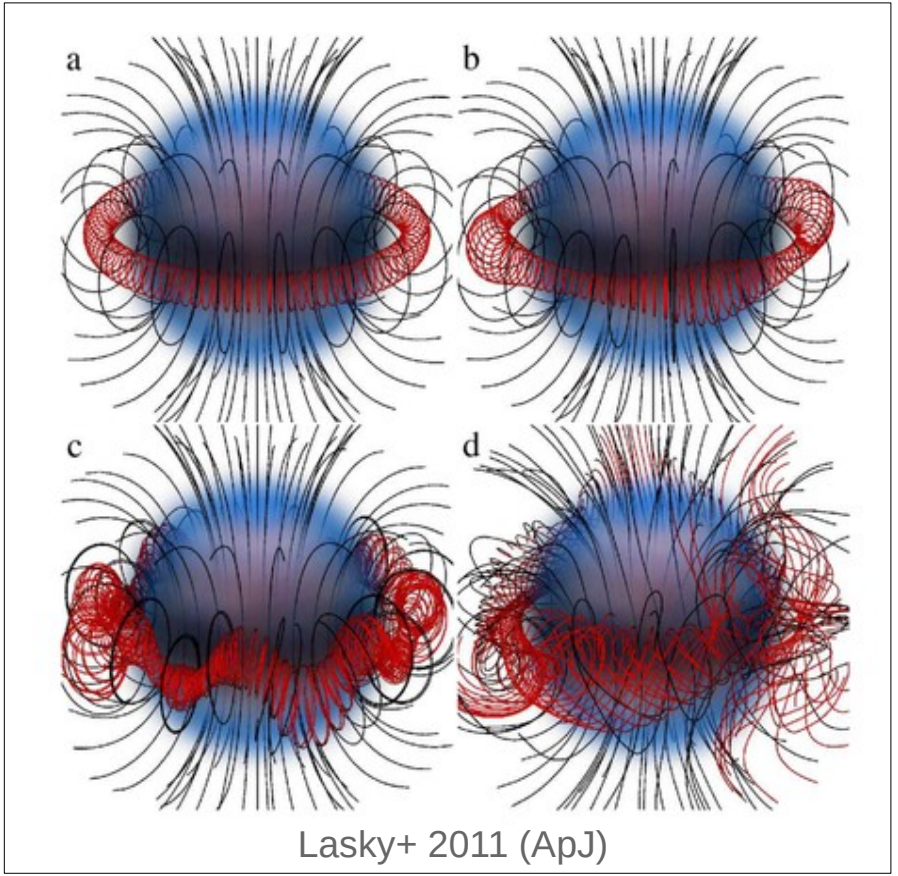

Lasky+ 2011 (ApJ)

Other MHD simulations

- PLUTO code: MHD simulations (both ideal and resistive), fiducial neutron star modeled with barotropic equation of state N=1 polytrope.
- Nonrotating star with mass=1.4 MSun and R=10 km, +atmosphere.
- Low resolution ~ 72x72x48.
- Two different initial conditions (from Haskell+, 2008):

  (1) Purely poloidal field

  (2) Mixed poloidal-toroidal field but with stronger toroidal part

- Surface field strength = 10^{16} G

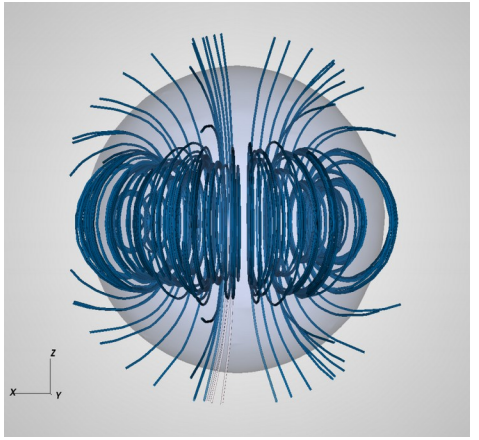

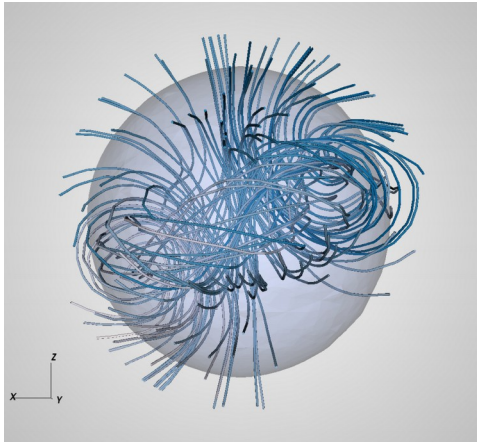

AS,BH,+ 2020 (MNRAS)

Dynamics

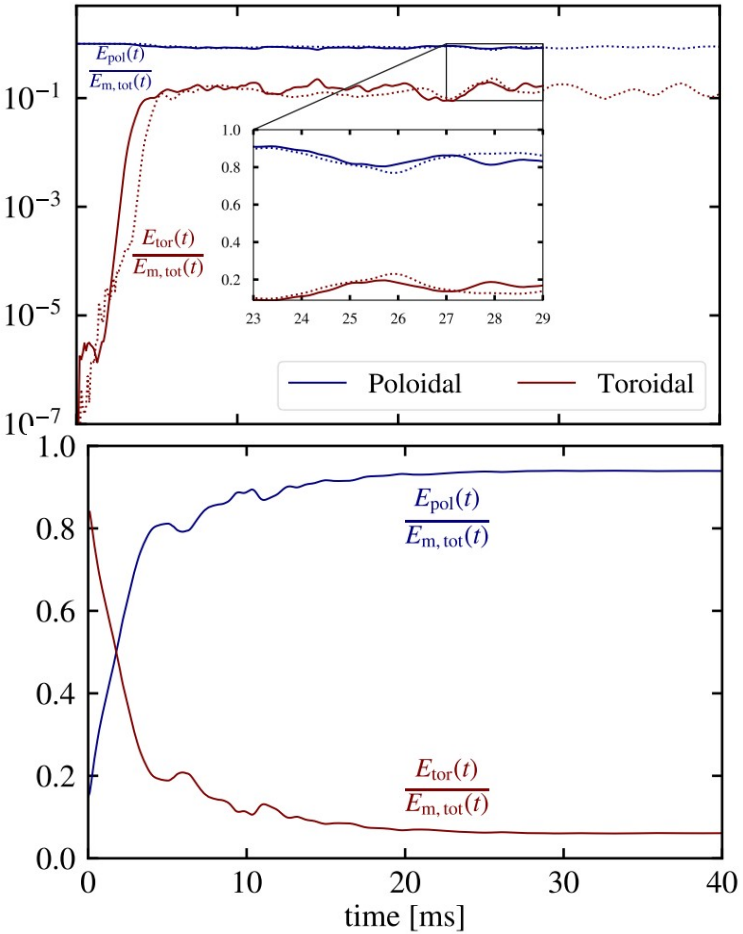

- Instability gives rise to toroidal field.
- Toroidal field undergoes exponential growth, becomes comparable in strength to the poloidal component.
- Growth timescale:

$$\tau_A = \frac{2R\sqrt{4\pi\langle\rho\rangle}}{\langle B\rangle}$$

- Poloidal and toroidal energies:

$$E_p = \int_V (B_r^2 + B_\theta^2) dV \qquad E_t = \int_V B_\phi^2 dV$$

- The poloidal field ~ (80-90)%, toroidal field ~ (10-20)%

AS,BH,+ 2020 (MNRAS)

Magnetic field lines

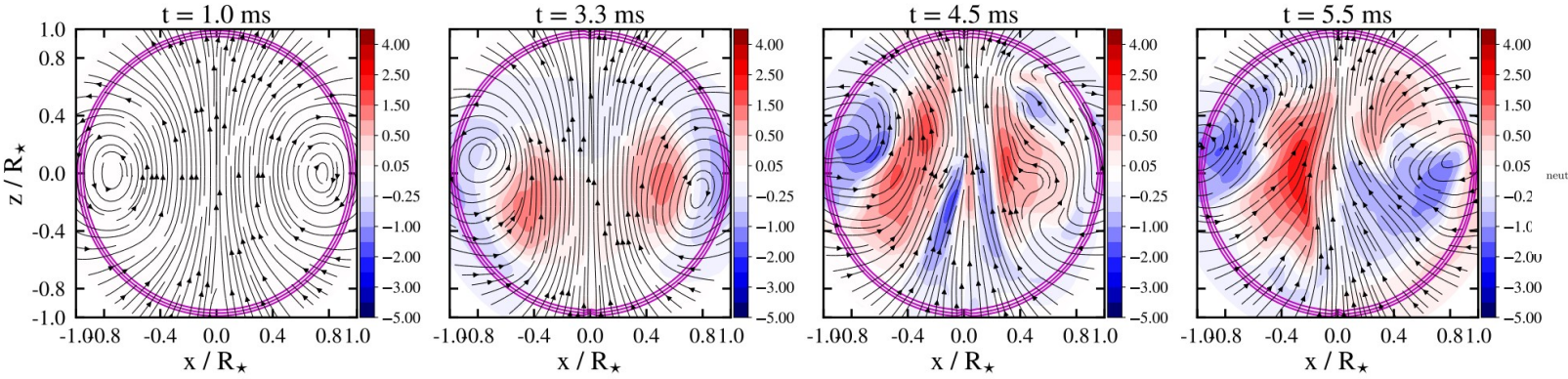

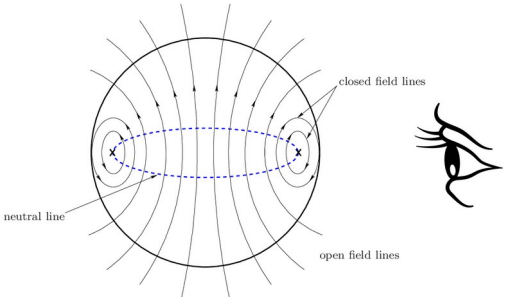

Side view

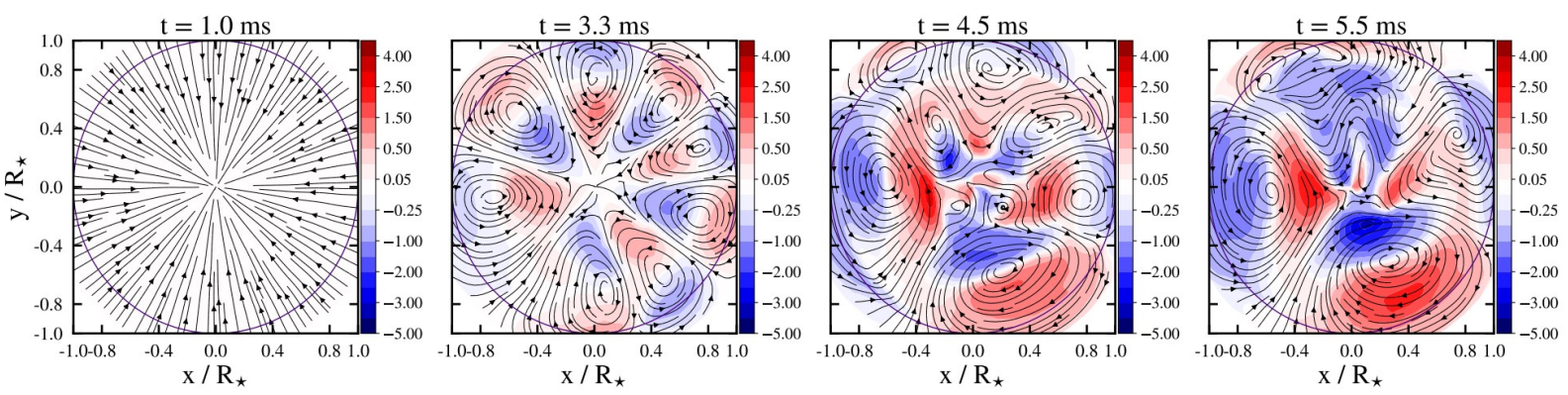

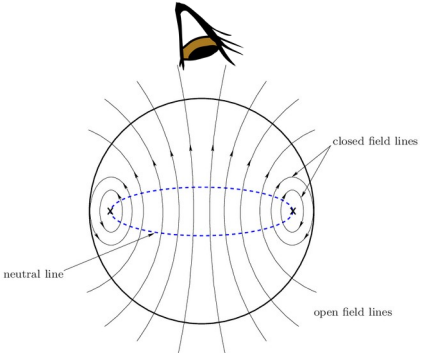

Top view

AS,BH,+ 2020 (MNRAS)

Visualizing kink instability

Neutral line

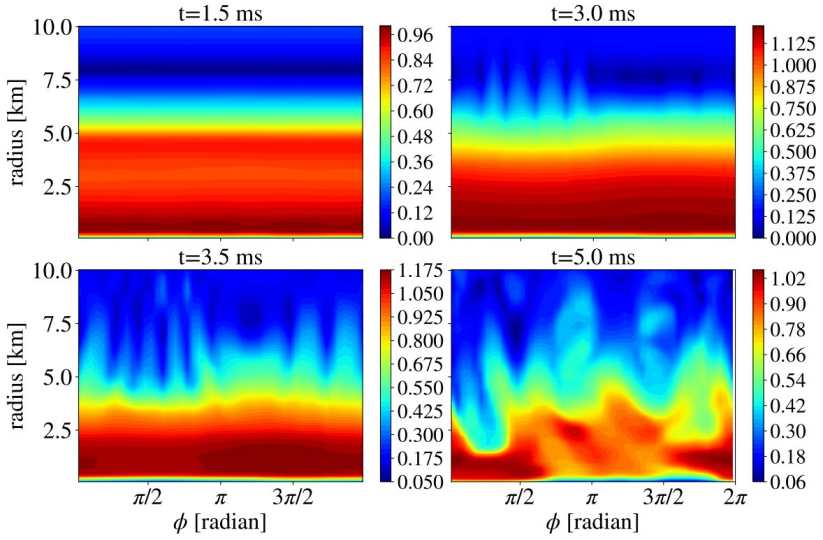

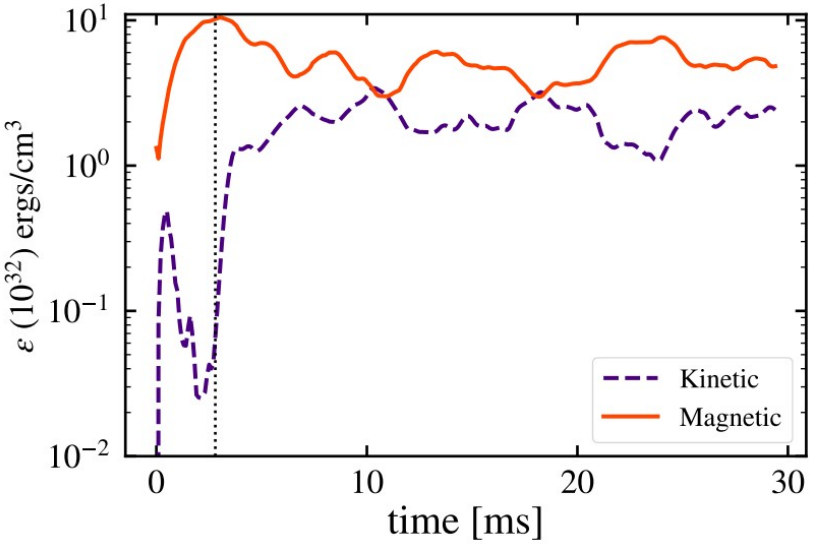

Kink instability = transverse displacements of a plasma column's cross-section from its center of mass without any change in the characteristics of the plasma.

AS,BH,+ 2020 (MNRAS)

Growth modes

AS,BH,+ 2020 (MNRAS)

- Fourier decomposition of the azimuthal component of the magnetic field into different modes of oscillations shows an exponential rise in strength for each component

$$C_m(B_\phi) = \int_0^{2\pi} B_\phi(\bar{\omega}, \phi, z=0) e^{im\phi} d\phi$$

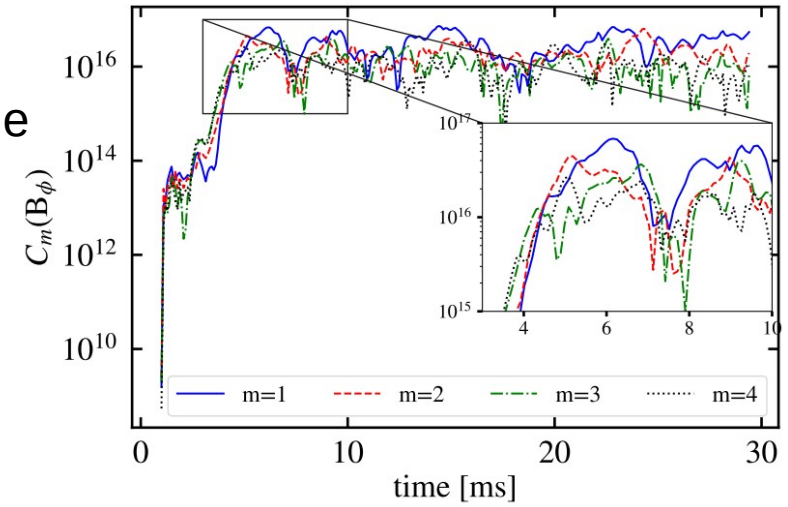

- The growth time can be calculated as

$$\tau_g = \frac{\Delta t}{\Delta \ln\left(C_m(B_\phi)\right)}$$

- Lower modes are stronger.

- Growth times reduce with increasing field strength.

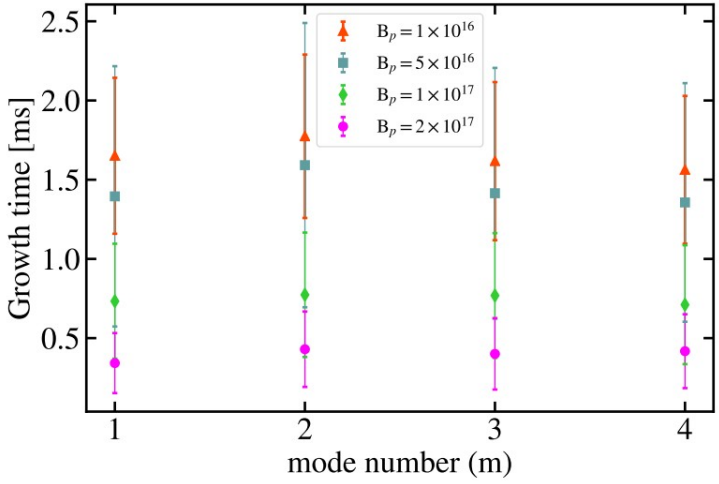

Problem set 10

Part a) Derive an expression for the characteristic age of pulsars assuming they are born rapidly rotating and spin down through magnetic braking in their lifetime. (2 points)

Part b) Using the ATNF Pulsar catalogue (https://www.atnf.csiro.au/research/pulsar/psrcat/), make a plot of the period and period derivative of the known pulsars. Draw the constant lines of the characteristic ages in the same plot. Also, explain what is the "death-line" of pulsars? (3 points)